Lasers in Surgery and Medicine 21:124–133 (1997)

In Vivo Light Transmission Spectra in EMT6/Ed Murine Tumors and Dunning R3327 Rat Prostate Tumors During Photodynamic Therapy

Åse M. Ballangrud, PHD,[1]* Oscar Barajas, MSC,[2] Alexia Georgousis, BPE,[1] Gerald G. Miller, PHD,[1] Ronald B. Moore, MD, PHD,[1] Malcolm S. McPhee, MD, MSC,[1] and John Tulip, PHD[2]

[1]Department of Surgery, Cross Cancer Institute, Edmonton, Alberta, Canada
[2]Departmentof Electrical Engineering, University of Alberta, Edmonton, Alberta, Canada

Background and Objective: **Variations in the optical coefficients in tissue and the photosensitizer during photodynamic therapy (PDT) will require adjustment of the light dose during the course of therapy. We have studied the dynamics using light transmission spectra for two different tumor models when tetrasulfonated aluminum phthalocyanine ($AlPcS_4$) was used as photosensitizer.**
Study Design/Materials and Methods: **Spectra were measured noninvasively in the EMT6/Ed murine tumor model, and with interstitially implanted source and probe fibers in the Dunning R3327-AT rat tumor model. Measurements were performed in the range 600–840 nm, using a tunable dye laser, a diode laser, and a Ti:Sapphire laser. $AlPcS_4$ has absorption in the range 600–700 nm with an absorption peak at 670 nm in saline.**
Results: **The in vivo spectrum of $AlPcS_4$ both in the EMT6/Ed tumor model and the Dunning R3327-AT tumor model differs from the spectrum of $AlPcS_4$ in saline. The absorption at 670 nm was reduced, whereas the absorption at 640 nm increased. Exposure of phototherapeutic levels of light caused reduced light absorption by the photosensitizer and further spectral shift.**
Conclusion: **We found that the $AlPcS_4$ absorption spectrum changes in a biological environment, and we also observed increased light transmission at the treatment wavelength during PDT in both tumor models. Instability in the absorption spectrum of the photosensitizer may influence the effectiveness of PDT. Lasers Surg. Med. 21:124–133, 1997.** **© 1997 Wiley-Liss, Inc.**

Key words: attenuation coefficient; photosensitizer absorption spectra; solid tumors; spectral shift; tetrasulfonated aluminum phthalocyanine; visible to near infrared spectra

INTRODUCTION

Successful treatment of solid tumors using photodynamic therapy (PDT) will require delivery of a sufficiently photoactivating light dose to all parts of the tumor. This requirement is difficult to achieve, because light transmission in tissue is limited, tumors are highly optically inhomogeneous and time changes of optical properties occur over the course of PDT. Light transmission in vivo can be very different from that in vitro. If the changes in light transmission are significant at the treatment wavelength, it will be necessary to

*Correspondence to: Åse M. Ballangrud, 436 East 69th Street, Apt. 12A, New York, NY 10021.

Accepted 25 September 1996.

develop methods to account for such variations during therapy.

Determination of the absorption and scattering coefficients in a scattering medium is complicated. For in vivo measurements, the optical coefficients may be determined by fitting a mathematical model that simulates light propagation, to experimental data [1–6]. In this work, we studied dynamic variations in the light transmission spectrum with time after drug injection and during PDT, and we have made no attempt to quantitatively determine the absorption and scattering coefficients. Brasseur et al. [7] has published in vivo absorption spectra of *bis*(dimethylthexylsiloxy)silicon 2,3-naphthalocyanine (SiNc8) in EMT6/Ed tumors at various times postinjection based on light reflection measurements. In vivo and *postmortem* light transmission measurements in muscle, liver, and brain have been published by Wilson et al. [8]. Optical coefficients have been determined in vivo in muscle with different doses of aluminum chlorosulphonated phthalocyanine (AlSPC), based on deformation of a laser pulse propagating through the tissue [9].

Phthalocyanines are promising photosensitizers for PDT of cancer that have received increasing attention because of their high absorption coefficient in the spectral range 650–680 nm where the penetration of light in tissue is high. Tetrasulfonated phthalocyanines have intense absorption in the near-infrared spectral range. Previous in vitro studies show that zinc tetrasulfonated phthalocyanine ($ZnPcS_4$) forms higher order aggregates in aqueous solution [10]. Monomeric $ZnPcS_4$ has a maximum at 670 nm, whereas the maximum in the absorption spectrum of dimers and larger aggregates is located at 640 nm. When the photosensitizer forms higher order aggregates or relocates in the cell over time, one cannot expect that their action spectra for photoinactivation of cells and sensitization of tumors parallel their monomeric absorption spectra. The influence of aggregated formations on the activation spectrum of sulfonated aluminum phthalocyanines is discussed by Moan et al. [11]. Excitation of the photosensitizer by low light levels is found to cause a redistribution of tetrasulfonated aluminum phthalocyanine ($AlPcS_4$) in the cell [12]. A spectral red shift is observed in the in vivo activation spectrum of other phthalocyanines like disulfonated aluminum phthalocyanine [13] and in zinc phthalocyanine tetrasulfonic acid [14].

The purpose of the experiment described here was to investigate in vivo changes in the light transmission spectra over the spectral range of 600–840 nm when tetrasulfonated aluminum phthalocyanine ($AlPcS_4$) was used as photosensitizer. Changes in the spectra were studied after the drug was administered to the animals and also during PDT. In vivo measurements of light transmission were performed with interstitially implanted source and probe fibers in the Dunning R3327-AT rat prostate tumor model and noninvasively in the EMT6/Ed murine tumor model.

MATERIALS AND METHODS

Setup

Light transmission was measured over the spectral range 600–840 nm using a dye laser (Coherent, Santa Clara, CA) tunable in the range 600–670 nm, a diode laser (SDL, Inc., San Jose, CA) at 688 nm, and a Ti:Sapphire laser (Spectra-Physics, Mountain View, CA) tunable over the spectral range 695–840 nm. The dye laser and the Ti:Sapphire laser were pumped by an argon-ion laser (Spectra-Physics Model 2580). The lasers were coupled to separate 400-μm-core diameter optical fibers with SMA fiber connectors at the distal end. The source fiber was switched between the lasers by switching the SMA connector between the fibers. The output power of the source fiber was in the range 10–300 mW, depending on wavelength. A shutter was used to block the laser beams to prevent illumination of the tissue for more than the 2 sec necessary for reading of the transmitted laser power. A schematic of the setup is shown in Figure 1.

The detector fiber was a flat cleaved optical fiber (flat ended fiber) with core diameter 400 μm. The numerical aperture of the flat cleaved fiber probe was 0.2 in air. The light collected by the flat cleaved fiber probe was detected by an integrating sphere with a silicon photodiode (United Detector Technology, Hawthorne, CA).

Light Transmission After Drug Administration

Changes in light transmission over time after injection of the photosensitizer were measured noninvasively in five mice with EMT6/Ed tumors by mounting the tumor between a flat cleaved source fiber and the flat cleaved probe fiber (Fig. 1a). Both fibers were touching the shaved skin over the tumor in a distance of 3–4 mm. The spectrum was measured prior to delivery of $AlPcS_4$ and then several times in the period from 1–52 hr after drug administration. Due to the frequency of

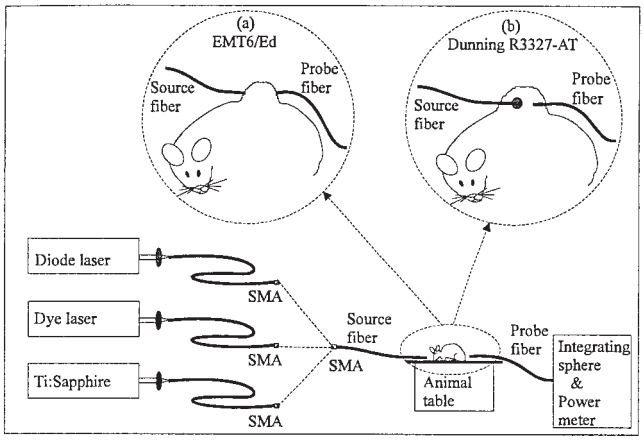

Fig. 1. Setup for measurement of in vivo light transmission. The light transmission was measured over the spectral range of 600–840 nm by using a dye laser tunable in the range 600–670 nm, a diode laser at 688 nm, and a Ti:Sapphire laser tunable over the spectral range 695–840 nm. The dye laser and the Ti:Sapphire laser were pumped by an argon-ion laser: **(a)** alignment of source and probe fiber for measurements in the EMT6/Ed tumors, **(b)** interstitial implanted source and probe fiber in the Dunning R3327-AT tumors.

these measurements and the length of this experiment, the animals were anesthetized for up to 15 min for each measurement by inhalation of Forane (Anaquest). Experiments were also performed in EMT6/Ed tumors where the mice were free of photosensitizer. Temporal variations in the spectra were measured in the murine EMT6/Ed tumors and not in the Dunning R3327-AT tumors since the spectra had to be measured several times over a 52-hr period, which was not possible in this tumor model requiring measurements with interstitially implanted fibers.

Light Transmission During PDT

Experiments were performed in five EMT6/Ed murine tumors and five Dunning R3327-AT rat tumors. The $AlPcS_4$ photosensitizer was administered intraperitoneally 26 hr prior to measurement of light transmission during PDT (25 mg/kg body weight). The light transmission was measured prior to illumination and then again after the tumor had been given a light dose of 300 J delivered at 100 mW (50 min). The treatment wavelength was 670 nm.

Light transmission was measured noninvasively in the murine EMT6/Ed tumors as described above and shown in Figure 1a. The mice were anesthetized for up to 90 min using intraperitoneal injection of Xylazine and Ketamine. It was important that they did not move during the experiment since that would have changed the alignment of the tumor relative to the source and probe fiber.

In the Dunning R3327-AT tumors, the spectra were measured with both the source fiber and the probe fiber interstitially implanted in the center of the tumor (Fig. 1b). The source was a diffusing tip of 3 mm diameter at the distal end of the fiber. A flat cleaved fiber was used as probe fiber. The fiber core diameter of both the source and the probe fiber was 400 μm. The probe fiber was oriented with the acceptance angle toward the source, 3 mm from the surface of the source. The rats were anesthetized for up to 90 min using intraperitoneal injection of Sodium Pentobarbital.

Light Transmission in Tissue Phantom

Temporal variations in the absorption spectrum of the tissue phantom, mixed with $AlPcS_4$, was measured with the spectrophotometer. Changes in the spectrum during PDT was measured with the tunable lasers in a tissue phantom mixed with $AlPcS_4$ before illumination and after 300 J were delivered to the phantom at 100 mW and 670 nm. The liquid phantom mixed with the drug was held in vessel such that none of the parameters were affected by the walls. The spherical diffusing fiber tip was used as source fiber, and the flat cleaved probe was positioned 3 mm from the source with the acceptance angle toward the source. Measurements of temporal variations and PDT induced changes were studied in four independent phantoms.

Fluorescence

The in vivo light transmission spectra were measured by tuning lasers over the spectral range 600–840 nm, without any optical filtering of the light detected. This means that in case of significant fluorescence from the photosensitizer the light intensity detected for a given laser wavelength will be higher than the actual transmitted light. A theoretical model simulating the contribution of fluorescent light and measurements of fluorescence from aluminum chlorosulfonated phthalocyanine (AlSPC) is published by Patterson et al. [15]. To test if fluorescent light would contribute to the results in our experiments, we compared the spectrum of the tissue phantom, mixed with 27 mg/l $AlPcS_4$, measured using three different techniques: (1) by using the tunable lasers as source and using a grating monochromator tuned to the corresponding source wavelength as filter prior to the detector, (2) by using the tunable la-

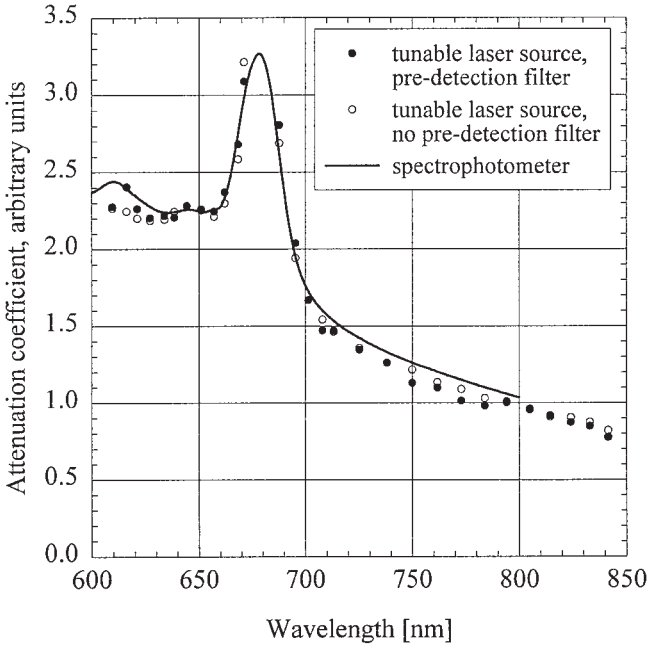

Fig. 2. Three different measurement techniques were compared to evaluate the influence of fluorescent light on the measured light transmission in a tissue phantom mixed with $AlPcS_4$. (●) Tunable lasers were used as source and a grating tuned to the corresponding source wavelength was used as filter prior to the detector. (○) Tunable lasers were used as source and both fluorescent and transmitted light were detected without any filtering prior to the detector. (—) The spectrum was measured with a spectrophotometer using a white light source and a grating prior to the detector to measure the transmitted and fluorescent light at each wavelength.

sers as source and detecting both fluorescent and transmitted light without any filtering prior to the detector, and (3) by using a spectrophotometer (Beckmann DU7400, Fullerton, CA), which is based on a white light source, and a grating prior to a detector array. To calculate the attenuation spectrum from methods (1) and (2), the measured light intensity at each wavelength in the tissue phantom mixed with $AlPcS_4$ was divided by the light intensity measured when water was used as sample. The measurements were performed with flat cleaved fibers both as source and probe fiber in the tissue phantom in a vessel such that none of the parameters were affected by the walls. Techniques (2) and (3) will both measure the transmitted and fluorescent light, whereas technique (1) will detect only transmitted light. This result is shown in Figure 2. The three measurement techniques all give the same spectrum, which means that the amount of fluorescent light does not significantly contribute to the spectral shift observed in the measured in vivo light transmission spectra. Therefore the light transmission spectra in the tumor models were measured without optical filtering prior to the detector.

Attenuation Coefficient

We measured dynamic variations in the light transmission spectrum and made no attempt to determine quantitatively the absorption and scattering coefficients in the tumor models. An attenuation coefficient, $\mu_t(\lambda)$, was calculated from the measured light transmission assuming that Beer's law applies:

$$\frac{I(\lambda)}{c\, I_0(\lambda)} = -\exp(-\mu,(\lambda)l), \qquad (1)$$

where $\mu_t(\lambda)$ is the wavelength-dependent light attenuation coefficient, l is the distance between the source fiber and the probe fiber, $I(\lambda)$ is the light intensity collected by the probe fiber and measured by the power meter at wavelength λ, $I_0(\lambda)$ is the incident light intensity from the source fiber, and c is the fraction of the light intensity emitted from the source fiber, which is collected by the probe fiber and detected on the photodetector. This fraction depends on the distance between the source and probe fiber, the numerical apertures of the probe fiber, the radiation field of the source fiber, and the refractive index of the medium (tissue). In the tissue phantom, the measured light transmission, $I(\lambda)$ can be divided by the measured light transmission in water, $c\, I_0(\lambda)$, to determine the fraction $I(\lambda)/(c\, I_0(\lambda))$. This cannot be determined accurately for the tumor measurements due to the higher refractive index of tissue compared to water. The coefficient c was estimated based on the tissue phantom measurements. Due to the uncertainty in this value, the decrease in attenuation coefficient with wavelength is not accurate. We have studied temporal variations and illumination induced variations in the photosensitizer's in vivo absorption spectrum. No attempt is made to quantitatively determine the attenuation coefficients.

For each experiment, the attenuation coefficient was scaled to unity at 840 nm where the photosensitizer has no absorption.

Photosensitizer

Tetrasulfonated aluminum phthalocyanine, $AlPcS_4$, was kindly supplied by Prof. Johan E. van

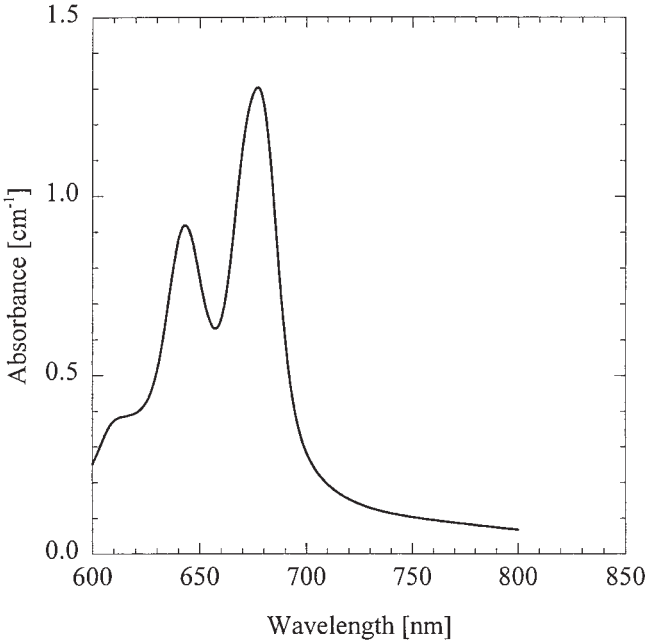

Fig. 3. Absorbance spectrum of 27 μg/ml $AlPcS_4$ in saline.

Lier (University of Sherbrooke, Québec). The synthesis and analysis of this drug are described by H. Ali et al. [16]. $AlPcS_4$ in saline has absorption in the spectral range 600–700 nm with a strong absorption peak in the red part of the spectrum at 670 nm. This is shown in Figure 3 for 27 μg/ml $AlPcS_4$ in saline. The solid compound was kept in the dark at 4°C. The $AlPcS_4$ was dissolved in 0.9% sodium chloride solution (Sigma Chemical Co., St. Louis, MO) immediately prior to intraperitoneal administration to the animals. The animal cages were covered to protect the animals from potential cutaneous photosensitization.

Tissue Phantom

The tissue phantom used in this experiment is described in a previous publication [17]. The phantom consists by volume of 1.73% Intralipid (10%, Kabi Pharmacia, Baie d'Urfe, Quebec), 0.18% Methylene Blue (1 μg/μl dissolved in distilled water) (Fisher Scientific, Fair Lawn, NJ) and 98.09% distilled water. At 630 nm, the Intralipid is highly forward scattering, and it has low absorption, similar to tissue. The light attenuation of the phantom was measured with a spectrophotometer, and at 630 nm the absorption coefficient of the phantom was determined as 0.25 cm^{-1}, with a reduced scattering coefficient of 7.0 cm^{-1}. This is a reduced scattering coefficient since the forward scattering in Intralipid will cause detection of some of the photons that have undergone scattering.

Tumor Models

Dunning tumors are considered to represent reasonable models of human prostate cancer [18–19]. The R3327-AT subline exhibits anaplastic histology, has a doubling time of 2–3 days and is relatively poorly perfused. The R3327-H tumor exhibits well differentiated histology, has a doubling time of 10–15 days, and is well perfused. In this experiment, only the R3327-AT subline was used. The tumors were maintained by serial transplantation of tumor fragments in the flanks of male Fisher × Copenhagen rat F_1 hybrids. The tumors are oblong in shape, with a maximum diameter of 25 mm.

EMT6/Ed murine tumor cells [20] are propagated in our laboratory both in vitro and in vivo. They are cultured in vitro as monolayers in plastic tissue-culture flasks in Waymounth's medium (GIBCO), serum (10% NU-serum + 2.5% fetal calf serum) and antibiotics (50 units/ml penicillin and 50 μg/ml streptomycin). Stock cultures are transferred twice weekly and display doubling times of 10–12 hr when incubated at 37°C in a water-saturated atmosphere of 95% air and 5% CO_2. This cell line is also passaged as solid tumors in BALB/c mice. The cells were implanted in the flank of the mice 1 week prior to the experiment. The tumors are spherical in shape, with a diameter of 6 mm.

RESULTS

Spectrum of $AlPcS_4$ in Tissue Phantom

The spectrum of $AlPcS_4$ mixed in the phantom (25 mg/ml) was measured with a spectrophotometer immediately after the drug was mixed with the phantom and then again 3 hr later. The mixture of phantom and $AlPcS_4$ was diluted a factor 1:4 in distilled water before the spectrum was measured. The solution was then exposed to room light over the 3-hr period. Figure 4 shows the absorbance spectrum just after the drug was mixed with the tissue phantom and 3 hrs after mixing. The solution was exposed to room light over the 3-hr period.

The spectrum is a combination of the $AlPcS_4$ absorption spectrum and the attenuation by the

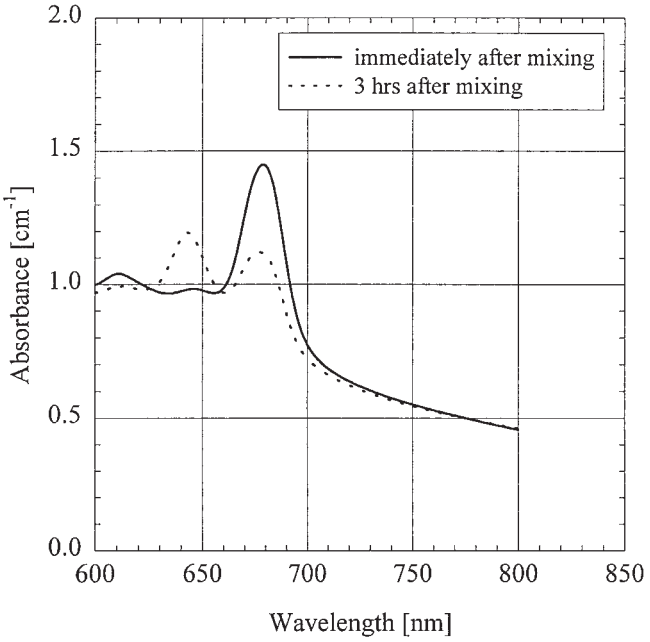

Fig. 4. Absorbance spectrum of 25 mg/l $AlPcS_4$ in the phantom, diluted a factor 1:4 in distilled water, immediately after mixing, and 3 hr after mixing.

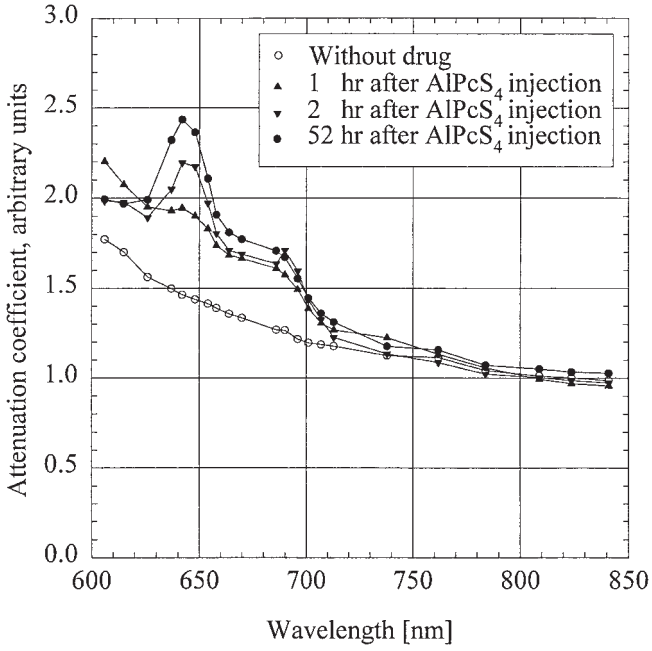

Fig. 5. In vivo attenuation spectrum in an EMT6/Ed tumor before injection of $AlPcS_4$, and then again 1 hr, 2 hr, and 52 hr after intraperitoneal injection of a concentration of 1.11 mg (50 mg/kg body weight) $AlPcS_4$ dissolved in 0.2 ml saline.

highly scattering phantom. Immediately after the drug was mixed with the phantom, the absorbance spectrum shows a peak at 670 nm. The spectrum changes over time and after 3 hr in room light the absorbance decreased at 670 nm and increased at 640 nm. We repeated the experiment except that the solution was kept in the dark at 4°C. Under these conditions, a similar change in the spectrum was observed, but it took place over a longer time. For example, it took 2 days to obtain a similar spectral shift as shown in Figure 4, which occurred after 3 hr.

In Vivo Spectrum of $AlPcS_4$ in EMT6/Ed Tumors

The light transmission spectrum was measured noninvasively in EMT6/Ed tumors as described above. The spectrum of the tumor was measured before $AlPcS_4$ was administered to the animal. A dose of 1.11 mg $AlPcS_4$ in 0.2 ml saline was administered by an intraperitoneal injection (50 mg/kg body weight), and the spectrum was measured 1 hr, 2 hr, and 52 hr after drug delivery. The same experiment was performed in a tumor where the animal was free of photosensitizer. From the measured light transmission data, an attenuation spectrum was calculated from equation (1). Since the exact same alignment could not be repeated for each measured spectrum, the spectra were scaled to unity at 840 nm where the drug has no absorption. The result is shown in Figure 5.

The absorption at 670 nm is relatively stable from 1 hr to 52 hr after drug administration, whereas the absorption at 640 nm increased with time.

In Vivo Spectrum of $AlPcS_4$ During PDT

EMT6/Ed tumor. The spectrum was measured before illumination, and then again after the tumors were given a light dose of 300 J, delivered at 100 mW and 670 nm. The same experiment was performed in EMT6/Ed tumors in animals free of $AlPcS_4$. This is shown in Figure 6 for a mouse given an intraperitoneal injection of 0.57 mg (25 mg/kg body weight) $AlPcS_4$ in 0.2 ml saline 26 hr prior to the experiment. The attenuation spectra from the tumor with and without drug were scaled to unity at 840 nm.

Reduced light attenuation in the spectral range 600–700 nm was observed in the animal with photosensitizer after delivery of a light dose of 300 J. Comparison of the spectra shows that the attenuation coefficient at 670 nm is reduced slightly relative to the attenuation coefficient at 640 nm after illumination.

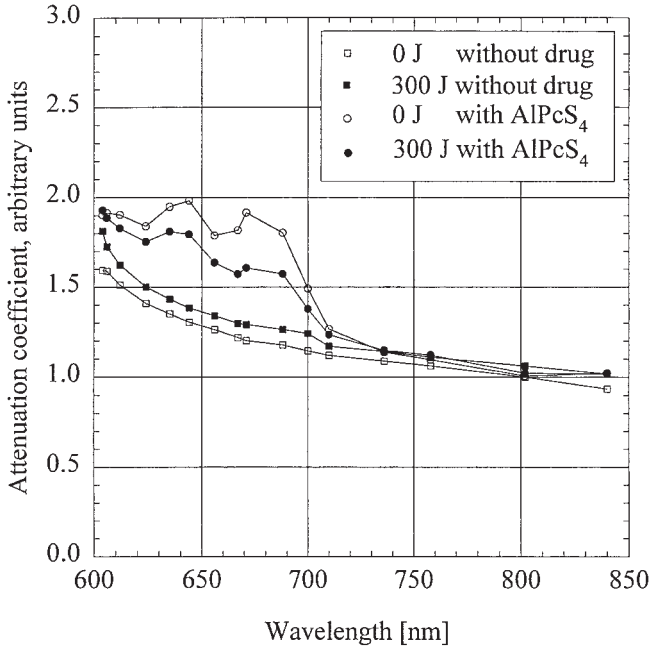

Fig. 6. In vivo attenuation spectrum of EMT6/Ed tumors before and after illumination. One animal was given 0.57 mg (25 mg/kg body weight) $AlPcS_4$ in 0.2 ml saline 26 hr prior to the experiment, and one animal was used as a blank without any photosensitizer. The spectrum was measured before illumination (0 J), and then again after the tumors were given a light dose of 300 J, delivered at 100 mW and 670 nm.

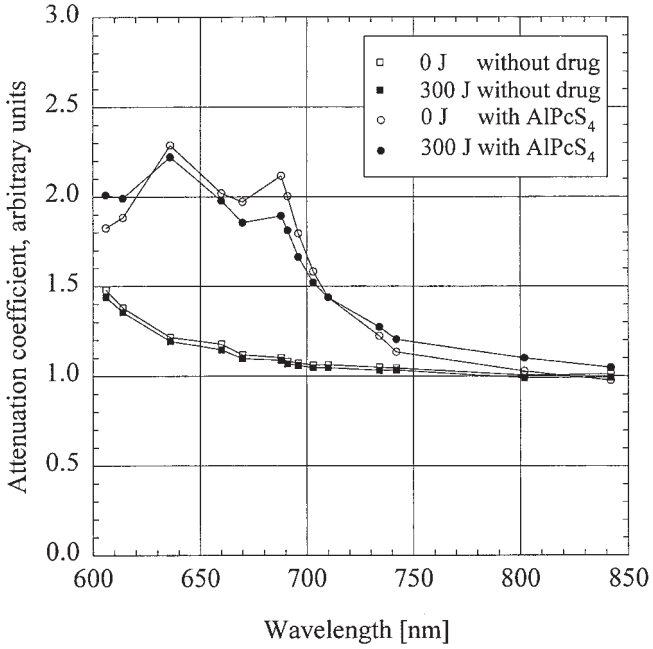

Fig. 7. In vivo measured attenuation spectrum in Dunning R3327-AT tumors before and after illumination. One animal was given an intraperitoneal injection of 12.79 mg (25 mg/kg body weight) $AlPcS_4$ in 0.2 ml saline 26 hr prior to the experiment, and one animal was used as a blank without any photosensitizer. The spectrum was measured before illumination (0 J) and then again after the tumor was given a light dose of 300 J at 100 mW and 670 nm.

Dunning R3327-AT tumor. The light transmission spectrum in Dunning R3327-AT tumors was measured with interstitially implanted fibers. The spectrum was measured before illumination, and again after the tumors were given a light dose of 300 J, delivered at 100 mW and 670 nm. This is shown in Figure 7 for a rat given an intraperitoneal injection of 12.79 mg (25 mg/kg body weight) $AlPcS_4$ in 0.2 ml saline 26 hr prior to the experiment. The spectrum was also measured in a Dunning R3327-AT tumor free of $AlPcS_4$. The attenuation spectra from the tumor with drug and the tumor without drug were scaled to unity at 840 nm.

The relative intensity of the attenuation at 670 nm and 640 nm was changed compared to the spectrum of $AlPcS_4$ in saline. A slight decrease in the light attenuation is observed at 670 nm during the course of therapy.

Tissue phantom. The light transmission spectrum was measured in a tissue phantom with and without $AlPcS_4$. A concentration of 13.5 mg (27 mg/l) $AlPcS_4$ was mixed with the phantom 2 hr prior to the experiment. The spectrum was measured, and then a light dose of 300 J was delivered at 100 mW and 670 nm to the solution. The same experiments was performed in a phantom free of photosensitizer. The result is shown in Figure 8.

DISCUSSION

All in vivo measurements of light transmission of $AlPcS_4$ in a biological environment and also in the lipid phantom solution show spectral changes compared to the spectrum in saline. The in vivo light transmission spectra in the EMT6/Ed tumor with $AlPcS_4$ shows that there was a spectral shift taking place overtime after the drug was administered to the animal (Fig. 5). Over the 52-hr period the light transmission was measured, the attenuation caused by the drug at 670 nm was unchanged, whereas there was increased attenuation at 640 nm.

The spectrum in the EMT6/Ed tumor during therapy using $AlPcS_4$ and 670 nm light (Fig. 6) shows that the ratio between the attenuation at 670 nm and 640 nm was reduced after 300 J was delivered at 100 mW to the tumor. We also see an

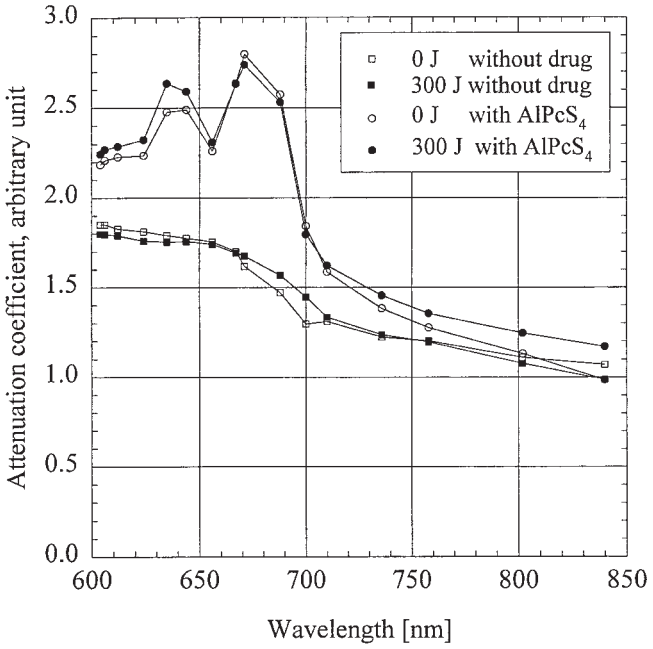

Fig. 8. Attenuation spectrum of a phantom with a concentration of 13.5 mg (27 mg/l) $AlPcS_4$ mixed with the phantom 2 hr prior to the experiment, and a phantom without photosensitizer. The spectra were measured before (0J) illumination with 670 nm light, and then again after a light dose of 300 J was delivered at 100 mW.

increased light transmission after illumination of the tumor in the spectral range where the photosensitizer has absorption. In the Dunning R3327-AT tumor, (Fig. 7), the light transmission was increased at 670 nm but not significantly at other wavelengths. Also in this tumor model, there was reduced attenuation at 670 nm relative to at 640 nm after illumination of the tumor.

The change in light transmission during illumination of the tumors may be caused by changes in the photosensitizer's absorption spectrum over time, or it may be accelerated by the light. The spectral shift occurring over time after drug administration (Fig. 5), was larger than the shift observed during PDT (Fig. 6). The experiments performed with $AlPcS_4$ in the phantom show that the spectral shift was accelerated by room light. Previously published data by Harriman et al. [10] on in vitro spectra of $ZnPcS_4$ show that $ZnPcS_4$ forms dimers and larger aggregates, and these heavier molecules have a slightly different absorption spectrum than the monomers. The change in the absorption spectrum of $AlPcS_4$ in a biological environment also may be caused by aggregation of $AlPcS_4$ after injection of the photosensitizer to the animal. For high concentrations (>25 μg/ml) of $AlPcS_4$, Peng et al. [12] have also shown that photo-excitation results in a relocation of the drug in the cell in vitro. In this same study, measurements of fluorescence intensity in cells before and after illumination also showed photobleaching of $AlPcS_4$.

The spectra in the Dunning R3327-AT tumor (Fig. 7) show an increased attenuation in the range 610–620 nm after illumination compared to before illumination. The measurements were performed with interstitially implanted source and probe fibers. After the experiment, the tumors were opened and we observed that blood accumulated around the fiber positions. The increased attenuation may be caused by blood coagulation during illumination.

For measurement of the light transmission spectrum during therapy, 300 J was delivered at 100 mW in both tumor models. The temperature was measured with needle thermocouples 3 mm from the source in a Dunning R3327-AT tumor and in the center of an EMT6/Ed tumor to see if the 100 mW power delivered to the tumor would cause temperature increase. There was no temperature increase in the Dunning R3327-AT tumor, but we observed a temperature increase of 6°C in the EMT6/Ed tumor when 100 mW was delivered to the surface of the tumor with a flat cleaved fiber.

The changes in light transmission overtime after administration of the photosensitizer required chronic anesthesia of the animals during the measurement, which took ~ 15 min. The animal was put back in the cage, and a new measurement performed some hours later. This introduced a new alignment for each spectrum. The attenuation spectra were scaled to unity at 840 nm. Whereas the fiber probes were not moved in the experiments observing changes induced by PDT, and the alignment was the same for all spectra measured in the same tumor. Since each individual spectrum measured in one tumor had the same alignment, the spectra for the given tumor were not normalized. However, when the spectra from different tumors are compared, they are scaled to overlap at 840 nm since the alignment differed for each tumor.

Illumination of the phantom mixed with the photosensitizer did not cause any change in spectrum at 670 nm, but a small increase in attenuation at 640 nm (Fig. 8). The measurements were performed 2 hr after $AlPcS_4$ was mixed with the phantom. The spectrum was similar to the

spectrum measured with the spectrophotometer 3 hr after the drug was mixed with the phantom (Fig. 4).

Each in vivo experiment was performed in a group of five animals, each carrying one tumor on the flank. The relative absorption caused by $AlPcS_4$ at 670 nm and 640 nm varied from animal to animal, but the shift in the spectrum, giving increased absorption at 640 nm and decreased absorption at 670 nm, was observed in all animals. We observed variations in the timescale for the shift to take place. This can be seen by comparing the spectrum of the EMT6/Ed tumor with $AlPcS_4$ (26 hr after injection) before illumination in Figure 6 with the spectra in Figure 5.

Some photosensitizers have strong fluorescence in the visible to near-infrared spectral range. We found that the amount of fluorescent light is negligible in our experiments, but wavelength selection prior to the detector is necessary for measurements where the distance between the source and probe fiber is so large that the transmitted light is attenuated to a level comparable to the amount of fluorescent light.

CONCLUSION

We observed dynamic variations in the in vivo light transmission spectra with time after administration of $AlPcS_4$. Dynamic variations in the absorption spectrum of $AlPcS_4$ during PDT may be caused by aggregation of the photosensitizer or a relocation in the cells after its administration to the animal. This process may be accentuated by the drug being exposed to therapeutic light levels. Study of in vivo absorption spectra of photosensitizers used for PDT is necessary to select an optimum treatment wavelength. Instability in the absorption spectrum of the photosensitizer may influence the accuracy of light dosimetry and the effectiveness of PDT.

ACKNOWLEDGMENTS

Financial support for this work was provided by the National Cancer Institute of Canada, Terry Fox Programme, the Alberta Heritage Foundation for Medical Research, and the Alberta Cancer Board. We thank Kevin Brown for maintaining the tumor models and for transplanting tumor fragments to the animals. Tetrasulfonated aluminum phthalocyanine was kindly supplied by Prof. Johan E. van Lier (University of Sherbrooke, Québec).

REFERENCES

1. Wilson BC, Patterson MS, Flock ST. Indirect versus direct techniques for the measurement of the optical properties of tissue. Photochem Photobiol 1987; 46(5):601–608.
2. Arnfield MR, Mathew RP, Tulip J, McPhee MS. Analysis of tissue optical coefficients using an approximate equation for comparable absorption and scattering. Phys Med Biol 1992; 37(6):1219–1230.
3. Arnfield MR, Chapman JD, Tulip J, Fenning MC, McPhee MS. Optical properties of experimental prostate tumors in vivo. Photochem Photobiol 1993; 57(2):306–311.
4. Pantelieds ML, Whitehurst C, Moore JV, King TA, Blacklock NJ. Photodynamic therapy for localised prostatic cancer: Light penetration in the human prostate gland. J Urol 1990; 143:398–401.
5. Whitehurst C, Pantelides ML, Moore JV, Brooman PJC, Blacklock NJ. In vivo laser light distribution in human prostatic carcinoma. J Urol 1994; 151:1411–1415.
6. Lilge L, Wilson BC. The accuracy of interstitial measurements of absolute light fluence rate in the determination of tissue optical properties. SPIE Laser-Tissue Interaction IV 1993; 1882:291–304.
7. Brasseur N, Ouellet R, Lewis K, Potter WR, van Lier JE. Photodynamic activities and skin photosensitivity of the *bis*(dimethylthexylsiloxy)silicon 2,3-naphthalocyanine in mice. Photochem Photobiol 1995; 62(6):1058–1065.
8. Wilson BC, Jeeves WP, Lowe DM. In vivo and post mortem measurements of the attenuation spectra of light in mammalian tissues. Photochem Photobiol 1985; 42(2): 153–162.
9. Patterson MS, Moulton JD, Wilson BC, Chance B. Applications of time-resolved light scattering measurements to photodynamic therapy dosimetry. SPIE Photodynamic Therapy: Mechanisms II 1990; 1203:62–75.
10. Harriman A, Richoux MC. Attempted photoproduction of hydrogen using sulfophthalocyanines as chromophores for three-component systems. J Chem Soc Farad Trans 1980; 76:1618–1626.
11. Moan J, Berg K, Bommer JC, Western A. Action spectra of phthalocyanines with respect to photosensitization of cells. Photochem Photobiol 1992; 56(2):171–175.
12. Peng Q, Farrants GW, Madslien K, Bommer JC, Moan J, Danielsen HE, Nesland JM. Subcellular localization, redistribution and photobleaching of sulfonated aluminum phthalocyanines in a human melanoma cell line. Int J Cancer 1991; 49:290–295.
13. Canti G, Lattuada D, Leroy E, Cubeddu R, Taroni P, Valentini G. Action spectrum of photoactivated phthalocyanine AlS_2Pc in tumor bearing mice. Anti Cancer Drug 1992; 3:139–142.
14. Griffiths J, Cruse-Sawyer J, Wood SR, Schofield J, Brown SB, Dixon B. On the photodynamic therapy action spectrum on zinc phthalocyanine tetrasulphonic acid in vivo. J Photochem Photobiol B: Biol 1994; 24:195–199.

15. Patterson MS, Pogue BW. Mathematical model for time-resolved and frequency-domain fluorescence spectroscopy in biological tissues. Applied Optics 1994; 33(10): 1963–1974.
16. Ali H, Langlois R, Wagner JR, Brasseur N, Paquette B, van Lier JE. Biological activities of phthalocyanines -X. Syntheses and analyses of sulfonated phthalocyanines. Photochem Photobiol 1988; 47(5):713–717.
17. Ballangrud ÅM, Wilson PJ, Brown K, Miller GG, Moore R, McPhee MS, Tulip J. Anisotropy of radiance in tissue phantoms and Dunning R3327 rat tumors: Radiance measurements with flat cleaved fiber probes. Lasers Surg Med 1996; 19:471–479.
18. Isaacs JT, Weissman RM, Coffey DS, Scott WW. Concepts in prostatic cancer biology: Dunning R3327-H, HI and AT tumors. Prog Clin Biol Res 1980; 37:311–323.
19. Lubaroff DM, Canfield L, Reynolds CW. The Dunning tumors. Prog Clin Biol Res 1980; 37:243–263.
20. Chapman JD, Baer K, Lee J. Characteristics of the metabolism-induced binding of misonidazole to hypoxic mammalian cells. Cancer Res 1983; 43:1523–1528.